SECOND EUROPEAN CONFERENCE ON EARTHQUAKE ENGINEERING
AND SEISMOLOGY, ISTANBUL AUG. 25-29, 2014

AN EFFICIENT ENERGY DISSIPATING DEVICE CALLED COMB-TEETH DAMPER

Sadegh GARIVANI[1], Ali Akbar AGHAKOUCHAK[2] and Sharif SHAHBEYK[3]

ABSTRACT

In this paper, a new type of yielding metallic damper called comb-teeth damper, CTD, is introduced. CTD is made of steel plates and includes a number of teeth that dissipate energy through in-plane flexural yielding. An optimum geometry of teeth is suggested, which assures uniform distribution of stress along them and prevents strain localization. Numerical FE modeling and test results are used to verify the design of proposed damper. Three full scale specimens have been made and tested under cyclic loading. The samples tolerated considerable cumulative displacement in their hysteresis cycles without any significant loss of strength. After these studies, the behavior of three simple steel frame equipped with proposed damper has been evaluated experimentally. The test results show that if this type of frames is designed appropriately, they can have a high energy dissipation capacity.

INTRODUCTION

Passive energy dissipation devices have been widely used in structures in the last decades, as effective and relatively low-cost systems to reduce the earthquake damage. Inelastic deformation of ductile metals in metallic dampers, sliding in friction dampers, flow of viscous fluids through narrow orifices in viscous dampers, and deformation of viscoelastic materials in viscoelastic dampers are some alternative mechanisms, which may be used to dissipate seismic energy (Soong and Spencer, 2002). Due to simpler manufacturing process, the yielding metallic dampers have found more widespread application in building construction compared to other types of energy dissipation systems.

The research on yielding metallic dampers was started by the pioneering works of Kelly et al. (1972), which was continuously followed by other researchers. Yielding metallic dampers, if effectively used, can dissipate significant portion of seismic energy through inelastic deformation of ductile metals. Generally, depending on the yielding mechanism, metallic dampers can be divided into four groups of flexural, axial, shear, and torsional.

The yielding dampers most widely used, are Added Damping and Stiffness, ADAS, Triangular-ADAS, TADAS (Bergman and Goel, 1987- Tsai et al., 1993- Xia et al., 1992) and Buckling restrained braces, BRBs (Wada and Nakashima, 2004- Tremblay et al., 2006). Yielding shear panels (Chana et al., 2009) and slit dampers (Jacobsen et al., 2010- Lee et al., 2002- Benavent, 2010- Li and Li, 2007- Chana and Albermani, 2008- Eatherton and Hajjar, 2010- Ghabraie et al., 2010- Oh et al., 2008) are other types of yielding dampers that are studied more recently.

Slit dampers are known as a special type of metallic dampers, in which plates with a number of slits or openings are subjected to in-plane shear deformations. The slits/openings divide the steel plate to a series of links acting in flexure under the global in-plane shear deformation of damper. Li and Li (2007) tested some slit dampers and applied them to a real structure. Based on the concept of slit dampers,

[1]Ph.D Candidate, TarbiatModares University, Tehran, s.gerivani@gmail.com
[2]Prof., TarbiatModares University, Tehran, a_agha@modares.ac.ir
[3]Assistant Prof., TarbiatModares University, Tehran, shahbeyk@modares.ac.ir

Benavent (2010) proposed and tested a new brace-type seismic damper. In addition to these researches, some attempts have been made to find the optimum geometry of openings. Studies of Chana and Albermani (2008), Ma et al.,(2010) and Ghabraei et al. (2010) can be referred in this regard.

In addition to the research conducted on identifying the characteristics of metallic yielding dampers, which has resulted in proposing many different types of these devices, some research have also been carried on the effects of these devices on seismic behavior of structures (Wittaker et al., 1991- Xia and Hanson, 1992- Aiken et al., 1993- Yamaguchi and El-Abd, 2003- Kasai et al., 2010). A review of literature in the field of metallic dampers and their applications in structures shows that this type of energy dissipation system has usually been used in moment resisting frames. As such if one is interested in using a damper in a steel frame with simple beam-to-column connections, the current literature do not explicitly address the needs.

Considering the results and observations of previous studies on slit dampers, this paper presents a new yielding metallic damper called comb-teeth damper, CTD, which consists of a series of steel links (or teeth) acting in parallel and dissipating energy through in-plane flexural yielding deformation. Special attention is paid to the geometric design of links in order to generate uniform stress distribution along their length and to prevent strain localization and premature failure. The design is then checked out through a set of nonlinear finite element analyses. After analytical and experimental studies on damper specimens, three simple steel frames equipped with proposed damper are also constructed and the cyclic behavior of them are evaluated.

COMB-TEETH DAMPER

Fig. 1(a) shows a typical comb-teeth damper, CTD, connecting a floor beam to a Chevron bracing in a building frame. The components of a CTD are shown in Fig. 1(b). As seen, a CTD is geometrically similar to half of a slit damper. The upper part of the steel plate is firmly bolted to the beam through a plate or T-shape section and horizontally aligned slotted holes are provided in the bottom plate that connects the links to the braces. This concept prevents axial forces to be generated in the links whereas enforces them to laterally act in parallel. Considering these connections, when a lateral deformation is applied to this frame, each link of damper is subjected to in-plane shear force as shown in Fig. 1(c) and dissipates energy through flexural yielding.

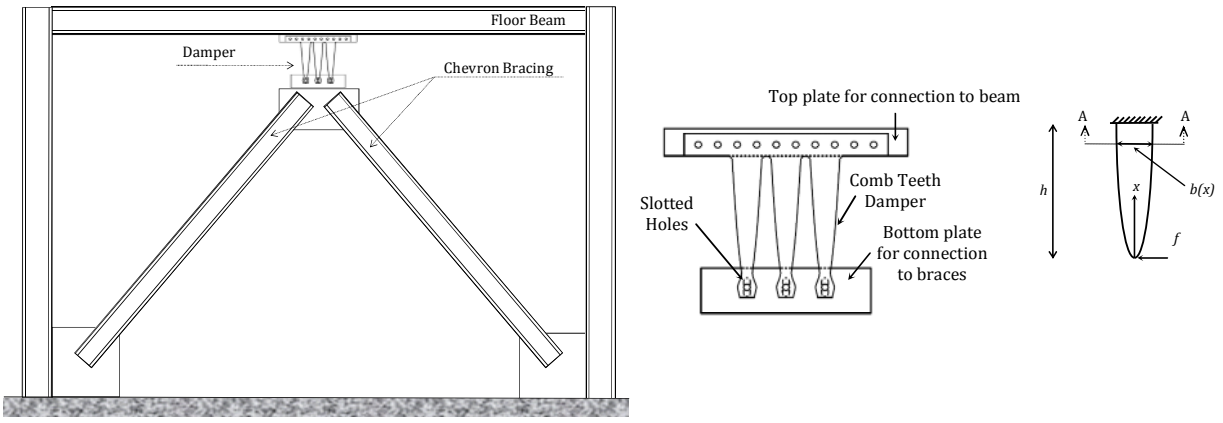

(a) (b) (c)

Figure 1. A typical slit damper in a frame, (a) Frame configuration, (b) Damper subjected to in-plane shear deformation, (c) Individual links of the damper.

Teeth shape design

Since the links of a CTD act in parallel, the global response of such damper can be estimated from the characteristics of an individual link (tooth). The shear force resisted by each link is trivially equal to $f = \frac{F}{n}$, where F and n are total damper shear force and the number of teeth, respectively. According to

the boundary conditions shown in Fig. 1 (c), this shear force introduces a linear variation of moment along the link. For an arbitrary section A-A in Fig. 1 (c), assuming Euler-Bernoulli beam theory, one can show

$$S(x) = \frac{tb^2(x)}{6} \tag{1}$$

$$\sigma(x) = \frac{M(x)}{S(x)} = \frac{6fx}{tb^2(x)} \tag{2}$$

Where x is the distance from the end of the link, t is the plate thickness and $b(x)$ is the width of the link at this section. $S(x)$ and $M(x)$ are corresponding elastic section modulus and applied moment, respectively. $\sigma(x)$ is the level of stress acting at the outer fiber of the section before yielding. As seen, all the characteristics of a link depend directly on $b(x)$ function, which defines the shape of link. From energy dissipation point of view, the optimum shape of link is the one that allows distributing induced inelastic deformations within the volume of material as evenly as possible. If it is assumed that

$$b(x) = 2\lambda\sqrt{x} \tag{3}$$

where λ is a constant, using Eq. (2) it is evident that $\sigma(x)$ is independent of x. In this case the outer fibers of the links of CTD reach yield stress simultaneously at any distance from the end and if the applied load is increased, the inelastic deformations are evenly spread towards the inner fibers of the section.

The elastic stiffness of an individual link, K_l^e, and also its yielding load, f_y, and yielding displacement, δ_y, can be calculated as below

$$K_l^e = \frac{Et\lambda^3}{h^{\frac{3}{2}}} \tag{4}$$

$$f_y = \frac{2}{3}t\lambda^2\sigma_y \tag{5}$$

$$\delta_y = \frac{2\sigma_y h^{\frac{3}{2}}}{3E\lambda} \tag{6}$$

where h and σ_y are link height and material yield stress, respectively. All above equations are based on the assumption that out of plane buckling of the links under bending does not occur and the behavior of the link follows the Euler-Bernoulli beam theory.

It should be noted that Fig.1 (c) shows the theoretical geometry of CTDs; however, as enough room is required to connect the damper to other structural parts, the width of the links could not be zero at their bottom ends and so, the damper should actually have a final shape shown in Fig.1 (b).

FEM ANALYSIS

Nonlinear finite element analysis is employed to verify the assumptions made for the design of CTDs and also the accuracy of the analytical equations presented in previous section. For the sake of simplicity, a single link (tooth) of a CTD is simulated in FEM. The values of coefficient λ, link heigth and thickness of plate are assumed equal to 1.75 $mm^{0.5}$, 235 mm and 10 mm, respectively.The material data obtained from a tensile coupon test are used to determine the material properties for FEM. According to test results, the modulus of elasticity and initial yield stress of the steel are equal to204 GPa and 274 MPa, respectively. The hardening response is approximated using a combined nonlinear isotropic-kinematic hardening model (Hibbitt et al., 2010).

The FE model of the link has been initially analyzed under monotonic loading. Fig. 2 shows the stress distribution of the link at three levels of applied lateral deflections. As seen, it confirms both simultaneous yielding of outer fibers and also uniform spread of plastic region within the link. The elastic stiffness, initial yield displacement, and yield strength are extracted and compared with those of analytical equations (Eqs. (4) to (6)) in Table 1. As the results are satisfactorily consistent, the obtained equations can be confidently used in the design process of parabolic links.

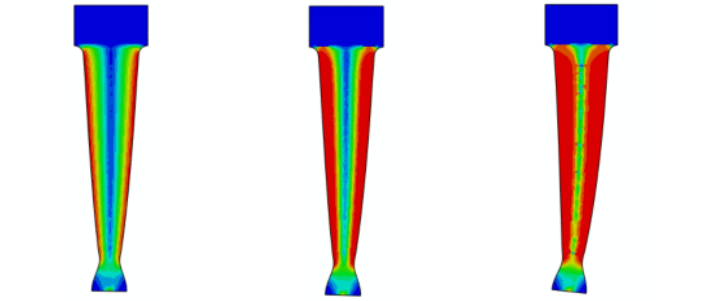

(a) End displacement=1.84 mm (b) End displacement=3.36 mm (c) End displacement=12.36 mm

Figure 2. Stress distribution along the linkin different stages of loading

Table 1. Characteristics of studied link obtained using two methods (units: N, mm)

Method	δ_y	K_l^e	f_y
Analytical Equations	1.89	2953	5594
FE Model	1.84	3028	5572

EXPERIMENTAL STUDY OF DAMPER SPECIMENS

In order to experimentally evaluate the behavior of proposed damper, three full scale specimens were made and loaded cyclically. The specimens were fabricated from a 10 mm thick structural steel plate using water jet cutting machine to avoid generation of significant residual stresses. The mechanical properties of steel were reported in previous section. The specimens included two layers each consisting of three links (teeth) with $h = 235$ mm and $\lambda = 1.75\ \text{mm}^{0.5}$.

Fig. 3 shows the designed test setup. As seen, the damper was installed between a reaction frame and a short loading column. For connecting the damper to reaction frame and short column, two T-shaped elements, marked as T1 and T2 in Fig. 3, were used. The two layers of CTDs were fastened to the sides of webs of T-shaped elements using high-strength grade 10.9 bolts. Slotted holes were provided in T1 element and the bolts were not pretensioned here to prevent generation of axial force in damper teeth.

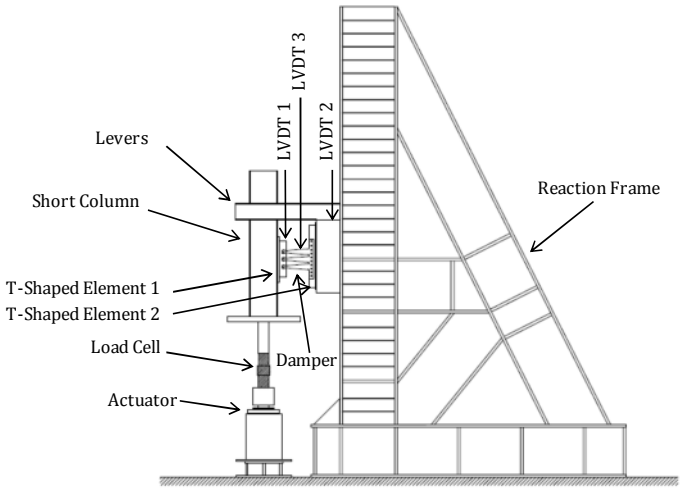

Figure3. Test Setup

A brittle coating of lime was applied to the surface of CTDs to follow the evolution of yielding pattern in the links. Displacement-controlled load was quasi-statically applied to the specimens by means of a 50 kN manual-controlled actuator. To prevent out-of-plane displacement of the

assemblage, two horizontal levers were provided (see, Fig. 3). Three LVDTs were also positioned to measure the relative in-plane shear displacement of the specimen and also the out-of-plane displacement of one of the links.

Specimen No. 1 (CTD1)

The displacement history applied to CTD1 and the recorded force-displacement curve are shown in Fig. 4(a) and 4(b), respectively. Yielding in damper started at a displacement of about 2 mm. As expected and depicted in Fig. 5, due to the uniformity of stress distribution along the links originated from special parabolic shape, outer fibers of the links yielded simultaneously. However, since out-of-plane displacements of the links were not restrained in CTD1, out-of-plane buckling of the links was observed as the applied in-plane shear deformation grew in sequential cycles (see, Fig. 6). The measurements of LVDT3 showed that the level of out-of-plane displacement in the links was significantly increased in the first 40 mm cycle, which was accompanied by strength reduction. This reduction continued till the end of tenth 40 mm cycle, when the strength decreased as much as 25 percent and the test was stopped. Although thoroughly checked at the end of test, no evidence of any cracking was found in the specimen. With respect to the yield displacement of about 2 mm, the amplitude of 40 mm corresponds to a ductility factor of $\mu \cong 20$.

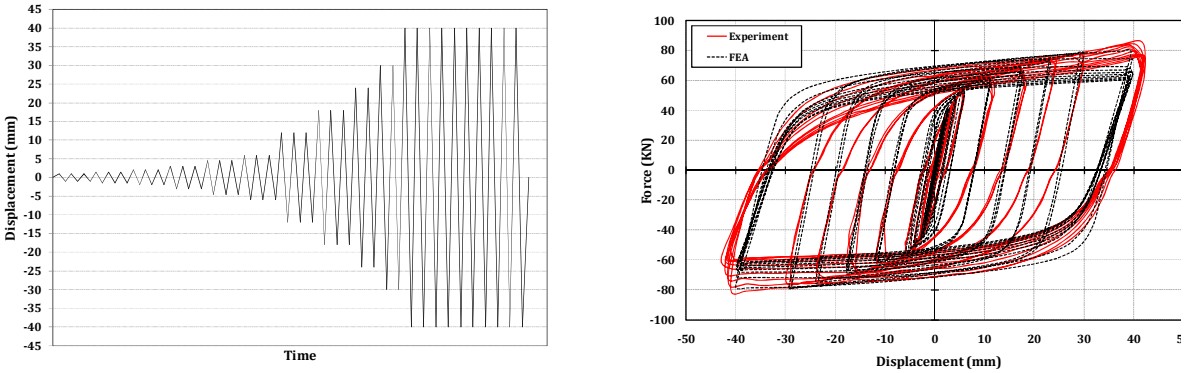

(a) (b)

Figure 4. (a) Displacement history of CTD1, (b) Force- displacement curves of CTD1; test results and FE analysis

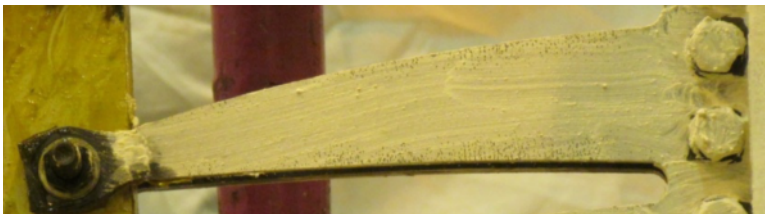

Figure 5. Simultaneous yielding of outer fibers along the links

Figure 6. Lateral buckling of the links (CTD1)

The FE model of CTD1 was also prepared and analyzed assuming an initial 1 mm imperfection proportional to the first out-of-plane buckling mode. The numerically calculated force-displacement curve of CTD1 is also reported in Fig. 4(b) which compares well with that of experiment. Furthermore, FEA correctly predicts the strength reduction in the same cycle as recorded in the test.

Specimen No. 2 (CTD2)

Observations on CTD1 revealed that, if no lateral restraints are provided, the links may experience out-of plane buckling. This phenomenon can adversely affect the behavior of damper especially its energy dissipation capacity and failure cycle. To resolve the problem, slight modification was made to the geometry of CTD2 by adding a restraining clamp to original design (see, Fig. 7(a)). The clamp consists of a 15 mm thick steel plate and two UNP60s. The steel plate was placed between the two layers of damper and then channel profiles were bolted together on both sides utilizing two additional teeth provided. It should be noted that the added clamp would not prevent in-plane movement of teeth. Displacement history applied to CTD2 is shown in Fig. 7(b). Good performance of clamp in preventing lateral buckling of links enabled damper to withstand many more cycles of loading in comparison to CTD1.

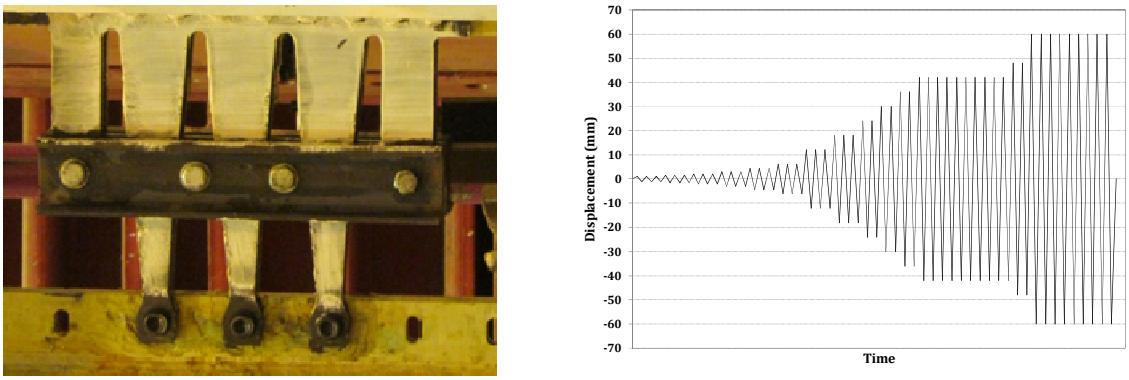

(a) (b)

Figure 7. (a) A view of CTD2, (b) Displacement history applied to CTD2

Stable hysteretic response of CTD2 can be seen in Fig. 8 (a). After ten cycles of 40 mm in amplitude, no strength degradation or fracture was observed. Thus, displacement amplitude was increased to 60 mm and test continued. The strength reduction began after sixth cycle at this amplitude and finally test stopped at ninth cycle of the same amplitude with the breakdown of one of links. The stable hysteretic behavior of this specimen is shown in Fig. 8 (b). The results show that CTD2 tolerated significant cumulative displacement of about 4100 mm before strength loss initiation.

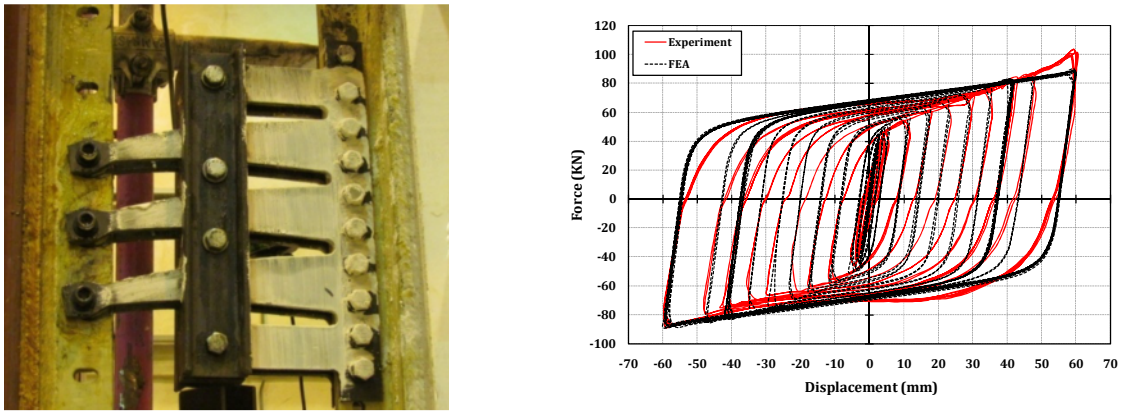

(a) (b)

Figure 8. (a) Specimen CTD2 during the loading, (b) Force- displacement curves of CTD2; test results and FE analysis

Specimen No. 3 (CTD3)

The results of CTD2 showed that the behavior of the proposed damper is satisfactory and hence it could be considered as an appropriate energy dissipating device in structures. According to the requirements of ASCE-41 (2006) and also FEMA356 (2000), such devices shall be loaded with 20 fully reversed cycles at a displacement corresponding to Maximum Considered Earthquake. Hence, the third specimen was fabricated identical to CTD2 but loaded under 20 fully reversed cycles at amplitude of 40 mm. Displacement history of CTD3 is shown in Fig. 9 (a). The behavior of specimen CTD3 was similar to that of CTD2. In this specimen, even after 20 cycles at amplitude of 40 mm, hysteretic curves were quite stable (see, Fig. 9 (b)) and thus displacement amplitude was increased to 60 mm. The cyclic loading was continued until the failure of one of the links at sixth cycle of this amplitude. The cumulative displacement tolerated by CTD3 was about 5000 mm. CTD3 was also simulated in FEM. The corresponding numerical force-displacement curve is also shown in Fig. 9 (b) and compared with that of experiment. Again, relatively good agreement has been observed.

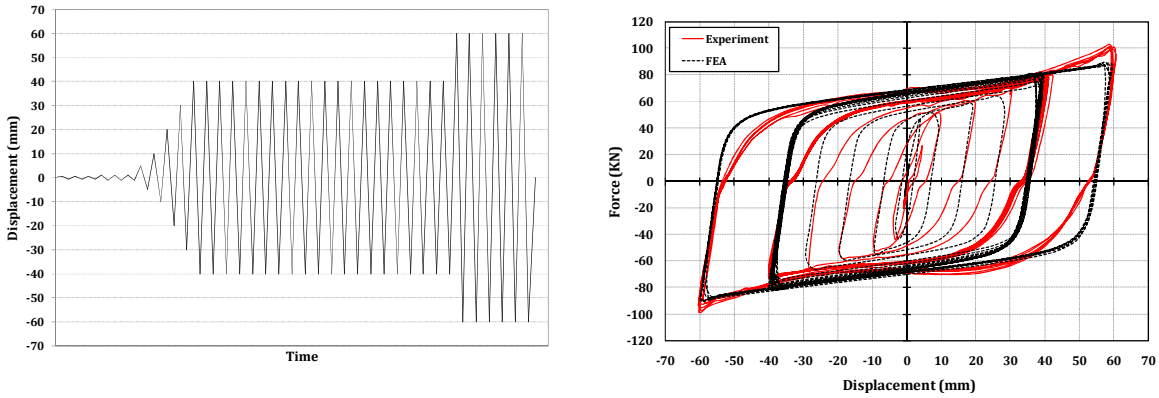

(a) (b)

Figure 9. (a) Displacement history applied to CTD3, (b) Force- displacement curves of CTD3; test results and FE analysis

As calculated analytically and observed experimentally, the yield displacement of the dampers is about 2 mm. So considering the displacement amplitude of 60 mm, a ductility ratio of about 30 is obtained. The backbone curve of CTD3 was also extracted and its equivalent bilinear curve was also plotted as shown in Fig. 10. In this bilinear curve, the yield displacement was about 2.7mm. Therefore, considering this effective yield displacement, the displacement amplitude of 40 mm corresponds to $\mu \cong 14.8$.

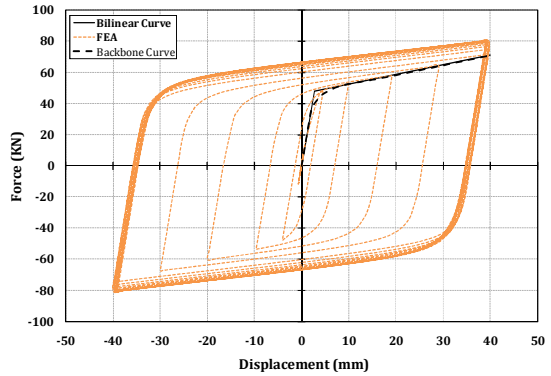

Figure 10. Backbone and bilinear curves of CTD3

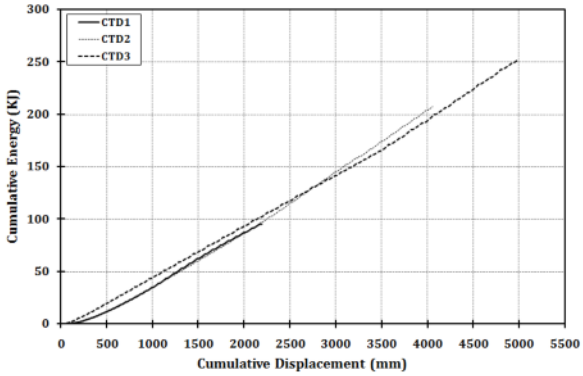

Figure 11. Cumulative dissipated energy versus cumulative displacement

The change of dissipated energy with increasing cumulative displacement is very similar for all three specimens (see Fig. 11). However, due to out-of-plane buckling of links in first specimen, the

maximum dissipated energy and maximum cumulative displacement of CTD1 differ significantly from those of CTD2 and CTD3. The maximum dissipated energy density is equal to $4.1 \times 10^{-4}\,\mathrm{kJ/mm^3}$ for CTD3 which is much greater than values reported for other types of slit dampers (Ghabraei et al., 2010).

EXPERIMENTAL STUDY OF THEFRAMES EQUIPPED WITH CTD

Since the behavior of CTDs proved to be satisfactory, three simple steel frames equipped with proposed damper were also tested. Fig. 12 (a) shows the experimental setup used in these tests. As seen in this figure, in order to prevent the out of plane displacement of the frame, the upper ends of the columns were restrained by two steel beams connected to the reaction frames. To measurement of relative displacements at different levels along the height, five LVDTs are used as shown in Fig. 12(b). Based on the performance philosophy of this type of structures, beams, columns and braces have been designed so that only the dampers would yield and other members remain elastic. Accordingly, the cross sections of beams, columns and braces are IPE270, IPB120 and 2UNP80, respectively. The gusset plates are designed based on the tension capacity of braces. Due to dimension limitations caused by the size of rigid base and reaction frames, tests were carried out on a half-scale steel frame. Since it was expected that the stiffness of simple steel frame would be negligible compared to the stiffness of combined braces and dampers, dampers were made full scale and installed in the frame. So basically the test frame was only geometrically half scale and the members were full scale. The horizontal cyclic loading was applied as displacement-control using two compressive jacks on both sides of the frame.

A view of the tested frame on the strong floor is shown in the Fig. 13. As shown, in order to prevent out-of-plane displacements of damper, two restrainers were installed on both sides of the dampers. Due to details of their connections to the frame, these restrainers do not cause any interference to in-plane displacement of damper.

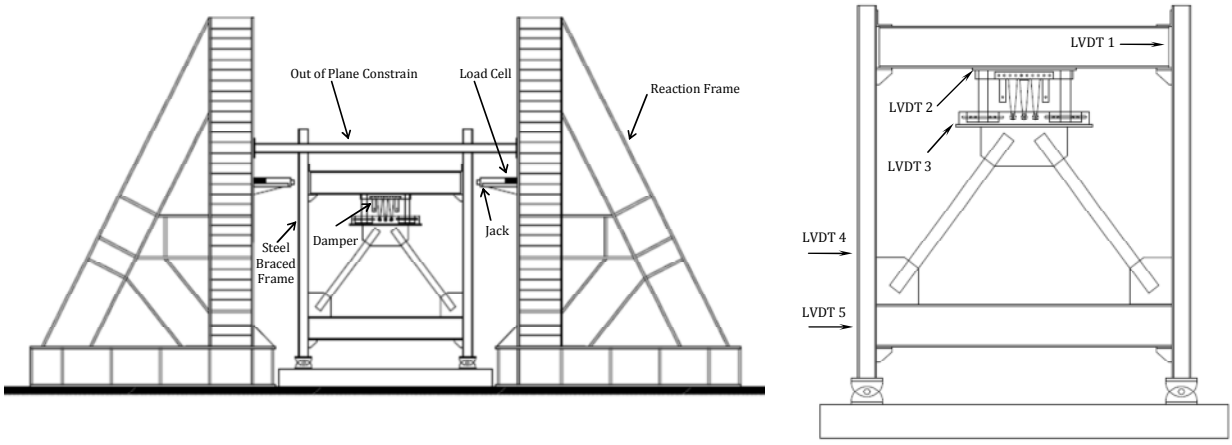

(a) (b)

Figure 12. Frame tests, (a) Experimental setup, (b) Location of mounted LVDTs

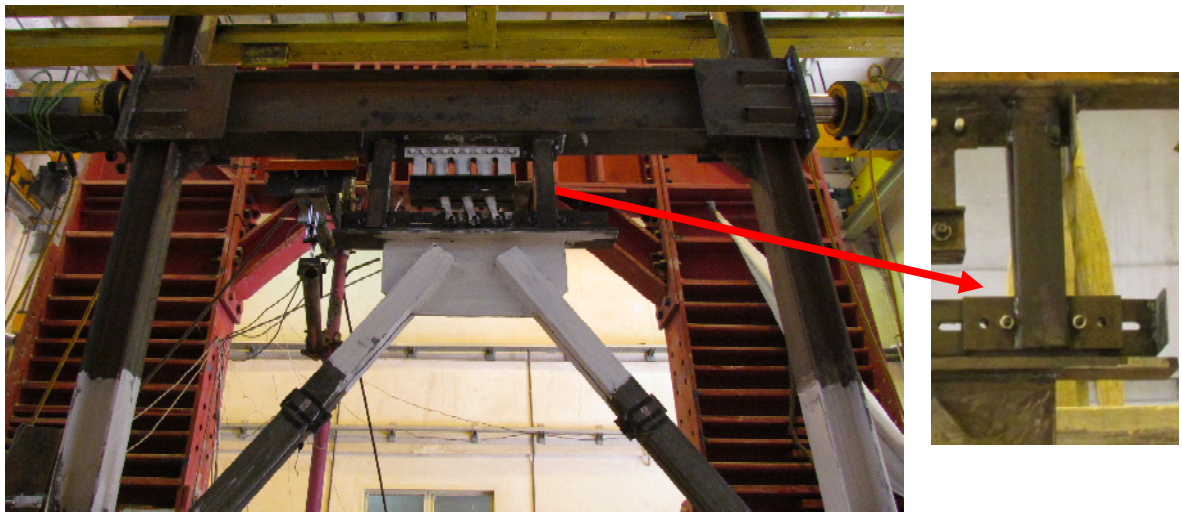

Figure 13. A view of studied steel frame equipped with CTD

Frame No. 1 (Fr.1)

The first tested frame (Fr.1) was equipped with a dampers identical to specimen No. 3 (CTD3) described in previous sections (Fig. 13).In this frame the bottom flanges of beams were connected to the columns using stiffened seated connection and the top flange of upper beam was connected using upper clip angle. In addition, the gusset plates of Chevron braces were fully welded to the beam and columns. The deformed shape of this frame during the loading is shown in Fig. 13. Simultaneous yielding of the outer fibers of the dampers teeth, appropriate performance of side restrainer and elastic behavior of braces were observed during this experiment. These observations also confirm the boundary conditions assumed in the experiments on damper specimens.

Despite the mentioned desirable performance of the damper and braces, the bottom beam-to-column connections showed a high level of fixity due to stiffened seated and fully welded gusset plates. During the cyclic loading, with increasing the level of story drift, this fixity caused yielding of the flanges of columns (Fig. 12 (a)), crack initiation in the welds of seated connection to beam (Fig. 12 (b)) and also yielding and finally fracture of the stiffener of stiffened seated connection (Fig. 12 (c)). It should be noted that this is a conventional connection type in braced frames, but as shown in Fig. 13, because of mentioned undesirable observations, the stiffness and strength of this frame decreased gradually after displacement amplitude corresponding to the drift angle of greater than 1.4%.

(a) (b) (c)

Figure 12. Undesirable observation in Fr.1, (a) Yielding of the flanges of columns, (b) Crack initiation in the welds of seated connection to beam, (c) Fracture of the stiffener of stiffened seated connection

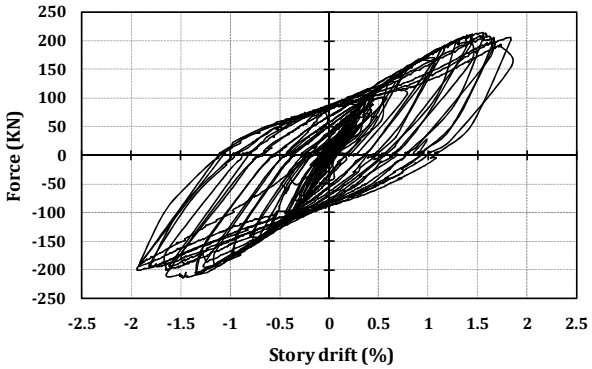

Figure 13. Force- displacement curve of Fr.1

Frame No. 2 (Fr.2)

Since the fixity of beam-to-column connections lead to relatively low ductility of the frame No.1, in the next experiment an attempt was made to reduce this fixity as much as possible. Fr.2 was also equipped with the same dampers. For this frame, the displacement was gradually increased and finally 10 cycles of loading were applied with anamplitude of displacement corresponding to adrift of 2.0%. The main difference between Fr.2 and Fr.1 was the beam-to-column and brace-to-frame connections. In Fr.2 two changes were appliedto reduce the fixity of beam-to-column connections. Firstly, the stiffened seated connection was replaced with web clip angles (Fig. 14 (a)) and secondly, the bracing gusset plates were not connected to columns (Fig. 14 (b)). These modifications lead to significant improvements in the behavior of Fr.2 compared with previous experiment. Fig. 15 shows force-displacement curve of this frame. As can be seen unlike Fr.1 (Fig. 13), there is no degradation in stiffness and strength of frame during the loading and Fr.2 has a very stable hysteretic behavior.

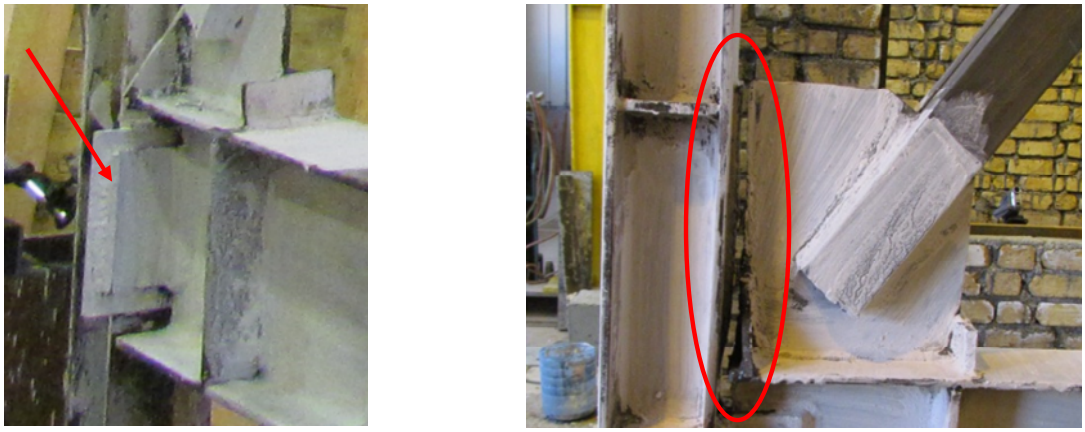

(a) (b)

Figure 14. Applied connection modifications in Fr.2, (a) Using web clip angles, (b) No connection between gusset plates and columns

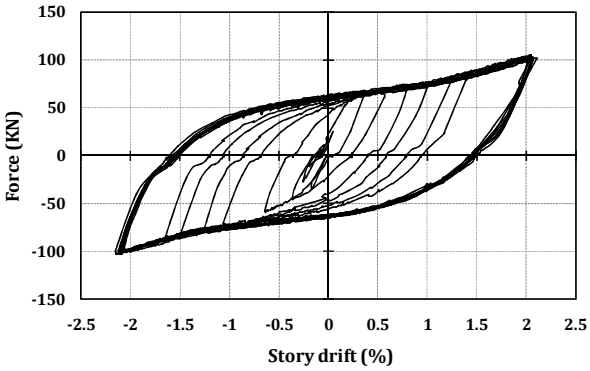

Figure 15. Force- displacement curves of FR. 2

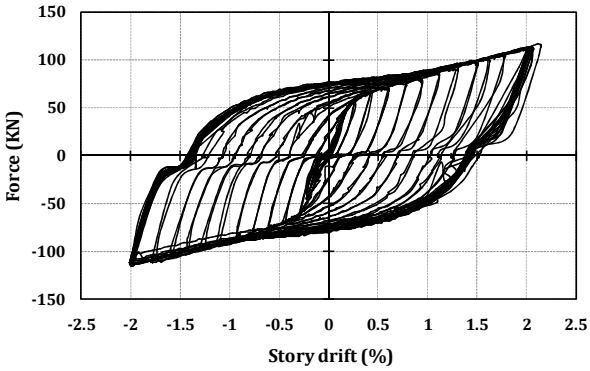

Figure 16. Force- displacement curves of FR. 3

Frame No. 3 (Fr3)

Fr.3 was also similar to Fr.2 in geometry and brace configuration but a new geometry of CTD wa used in this experiment. This damper included two layers each consisting of two links (teeth) with $h = 235\ \text{mm}$ and $\lambda = 2.5\ \text{mm}^{0.5}$ (Fig. 17). In this experiment the displacement amplitude was also gradually increased to reach a value corresponding to storey drift of 2% and then 20 cycles of loading were applied in this amplitude. Fig. 16 shows the force-displacement curve of Fr.3. This frame has a very stable hysteresis curve and hence is consistent with the design assumptions and goals. It should be noted, the maximum displacement amplitude of damper in Fr.3 was equal to 35 mm. Based on the verified analytical equations (Eq. (6)), the yield displacement of this damper is equal to 1.3 mm. It means that Fr.3 tolerated 20 cycles of loading with a displacement amplitude corresponding to ductility factor equal to $\mu \cong 27$, which is a significant value of ductility capacity..

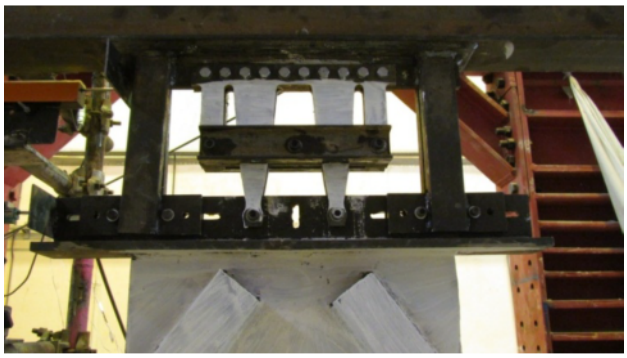

Figure 16. A view of Fr.3 with a new geometry of CTD

CONCLUSIONS

In this paper a new type of yielding metallic damper named comb-teeth damper, CTD, is presented. Numerical and experimental results show that the special design of connections of CTDs (slotted holes) effectively prevents the generation of undesirable axial load in links. In addition, the parabolic shape proposed for the links of CTDs leads to uniform stress distributionalong their length and prevents strain localization and premature failure. This guarantees high energy dissipation capacity and ductility of links. For instance CTD3 specimen tolerated approximately 5000 mm of cumulative displacement and dissipated $4.1 \times 10^{-4}\ \text{kJ/mm}^3$ energy.

In order to evaluate the cyclic behavior of frames equipped with proposed damper, three frames were also tested. A restrainer was also designed to prevent the overall out-of-plane deformation of the

dampers. The results of these experiments confirmed that such frames can dissipate significant amount of input energy with stable hysteretic behavior.

REFERENCES

Aiken ID, Douglas KN, Whittaker AS, Kelly JM (2003) "Testing of passive energy dissipation systems", *Earthquake Spectra*, 9:335-70

American Society of Civil Engineers (2006), Seismic Rehabilitation of Existing Buildings, ASCE/SEI 41-06

Benavent-Climent A (2010) "A brace-type seismic damper based on yielding the walls of hollow structural sections", *Engineering Structures*, 32:1113-22

Bergman DM, Goel SC (1987) "Evaluation of cyclic testing of steel plate device for added damping and stiffness", Report No. UMCE 87-10, The University of Michigan, Ann Arbor, MI

Chana RWK, Albermani F, Williams MS (2009) "Evaluation of yielding shear panel device for passive energy dissipation", *Journal* of *ConstructionalSteel Research*, 65:260-8

Chana RWK, Albermani F (2008) "Experimental study of steel slit damper for passive energy dissipation", *Engineering Structures,* 30:1058-66

Federal Emergency Management Agency (2000), Prestandard and Commentary for the Seismic Rehabilitation of Buildings, FEMA 356

Ghabraie K, Chan R, Huang X, Xie YM (2010) "Shape optimization of metallic yielding devices for passive mitigation of seismic energy", *Engineering Structures,* 32:2258–67

Hibbitt, Karlsson, and Sorensen Inc, ABAQUS User's manual version 6.10 (2010),

Kasai K, Ito H, Ooki Y, Hikino T, Kajiwara K, MotoyuiSh, Ozaki H, Ishii M (2010) "Full-scale shake table tests of 5-story steel building with various dampers", *Proceedings 7th International Conference on Urban Earthquake Engineering & 5th International Conference on Earthquake Engineering*, Tokyo, Japan, 3-5March, 11-22.

Kelly JM, Skinner RI and Heine AJ (1972) "Mechanisms of energy absorption in special devices for use in earthquake resistant structures", *Bull NZ Nat Soc Earthquake Engineering,* 5:63-88

Lee MH, Oh SH, Huh C, Oh YS, Yoon MH, Moon TS (2002) "Ultimate energy absorption capacity of steel plate slit dampers subjected to shear force", *International Journal of Steel Structure,* 2:71-9

Li HN, Li G (2007) "Experimental study of structure with dual function metallic dampers", *Engineering Structures*, 29:1917-28

Ma X, Borchers E, Pena A, Krawinkler H, Billington S, Deierlein GG (2010) "Design and behavior of steel shear plates with opening as energy dissipating fuses", Report No. 173, The John A. Blume Earthquake Engineering Center

Oh SH, Kim YJ, Ryu HS (2009) "Seismic performance of steel structures with slit dampers", *Engineering Structures*, 31:1997-2008

Soong TT, Spencer BF (2002) "Supplemental energy dissipation: state of art and state of the practice",*Engineering Structures*, 24:243-59

Tremblay R, Bolduc P, Neville R, Devall R (2006) "Seismic testing and performance of buckling-restrained bracing systems", *Canadian Journal* of *Civil Engineering,* 33:183-98

Tsai KC, Chen HW, Hong CP, Su YF (1993) "Design of steel triangular plate energy absorbers for seismic-resistance construction", *Earthquake Spectra*, 9:505-28.

Wada A, Nakashima M (2004) "From infancy to maturity of buckling restrained braces research", *Proceedings 13th World Conference on Earthquake Engineering,* 1-6 August, Canada, Vancouver, Paper No. 1732

Wittaker AS, Bertero VV, Thompson CL, Alonso LJ (1991) "Seismic testing of steel plate energy dissipation devices", *Earthquake Spectra*, 7:563-604.

Xia C, Hanson R (1992) "Influence of ADAS Element Parameters on Building Seismic Response", *ASCE Journal of Structural Engineering*, 118:1903-18

Yamaguchi H, El-Abd A (2003) "Effect of earthquake energy input characteristics on hysteretic damper efficiency", *Earthquake Engineering & Structural* Dynamics, *32*:827–43